A&A 520, A113 (2010)
DOI: 10.1051/0004-6361/201014248

Astronomy & Astrophysics

VLBI observations of optically-bright extragalactic radio sources for the alignment of the radio frame with the future Gaia frame

I. Source detection⋆

G. Bourda[1,2], P. Charlot[1,2], R. W. Porcas[3], and S. T. Garrington[4]

[1] Université de Bordeaux, Observatoire Aquitain des Sciences de l'Univers, 2 rue de l'Observatoire, BP 89, 33271 Floirac Cedex, France
e-mail: bourda@obs.u-bordeaux1.fr
[2] CNRS, UMR 5804, Laboratoire d'Astrophysique de Bordeaux, 2 rue de l'Observatoire, BP89, 33271 Floirac Cedex, France
[3] Max-Planck-Institut für Radioastronomie, Auf dem Hügel 69, 53121 Bonn, Germany
[4] University of Manchester, Jodrell Bank Observatory, Macclesfield, Cheshire SK11 9DL, UK

Received 11 February 2010 / Accepted 1 July 2010

ABSTRACT

Context. The European space astrometry mission Gaia will construct a dense optical QSO-based celestial reference frame. For consistency between optical and radio positions, it will be important to align the Gaia and VLBI frames with the highest possible accuracy. It has been found that only 70 (10%) of the sources from the International Celestial Reference Frame (ICRF) are suitable for establishing this link, either because they are not bright enough at optical wavelengths or because they have significant extended radio emission which precludes reaching the highest astrometric accuracy.
Aims. In order to improve the situation, we have initiated a VLBI survey dedicated to finding additional suitable radio sources for aligning the two frames.
Methods. The sample consists of 447 optically-bright (magnitude ≤18) extragalactic radio sources, typically 20 times weaker than the ICRF sources, which have been selected by cross-correlating an optical quasar catalog with the NRAO VLA Sky Survey (NVSS).
Results. This paper presents the observing strategy to detect, image, and measure accurate radio positions for these sources. It also provides results on the VLBI detectability of the sources, as derived from initial observations with the European VLBI Network in June and October 2007. Based on these observations, a high detection rate of 89% is found, which is promising for the continuation of this project. This high VLBI detection rate for sources from the NVSS catalog is probably due to the selection process, suggesting that optically-bright quasars have compact radio structures.

Key words. reference systems – quasars: general – astrometry – catalogs – methods: observational – techniques: interferometric

1. Introduction

During the International Astronomical Union (IAU) 23rd General Assembly, in Kyoto (Japan) in August 1997, it was decided that the fundamental celestial reference system (ICRS; International Celestial Reference System; Arias et al. 1995) would be realized based on positions of extragalactic sources. The celestial reference frame, its practical realization, is dedicated to permitting the location of any celestial target in the Universe. It is defined by a set of positions of celestial objects, which allow a formal determination of the origin and orientation of the frame. The celestial reference frame is crucial, and widely used in the field of astronomy and astrophysics for a number of applications (e.g. spacecraft navigation in the solar system, proper motion studies within the Galaxy and the Local Group, multi-wavelength studies to constrain astrophysical models of celestial objects). The first ICRS realization at radio wavelengths, the International Celestial Reference Frame (ICRF), comprises the positions of 608 extragalactic radio sources (Ma et al. 1998), with supplementary positions for 109 sources added in a second stage (Fey et al. 2004). The coordinates of these radio sources were estimated through Very Long Baseline Interferometry (VLBI) measurements, from dual-frequency S/X observations (2.3 and 8.4 GHz), with a noise floor of 250 microarcseconds (μas). The second realization of the ICRS, the ICRF2 (see IERS Technical Note 35, 2009), was adopted during the IAU 27th General Assembly in Rio de Janeiro (Brazil), in August 2009. The ICRF2 consists of a catalog with the VLBI coordinates of 3414 extragalactic radio sources (from which 295 are *defining* sources). It was constructed from all geodetic and astrometric VLBI data acquired so far, including those from the Very Long Baseline Array (VLBA) Calibrator Survey (VCS; Beasley et al. 2002; Fomalont et al. 2003; Petrov et al. 2005, 2006; Kovalev et al. 2007; Petrov et al. 2008). It has a noise floor in position of about 60 μas and an axis stability of 10 μas.

The European Space Agency (ESA) space astrometric mission Gaia, to be launched in 2012, will survey all stars and QSOs (quasi stellar objects) brighter than magnitude 20 (Perryman et al. 2001). Based on current estimates from local surveys, it is anticipated that 500 000 such QSOs should be detected. Optical positions will be determined with Gaia with an unprecedented

⋆ The entire list of radio sources detected (i.e. complete Table 3) is only available in electronic form at the CDS via anonymous ftp to cdsarc.u-strasbg.fr (130.79.128.5) or via http://cdsarc.u-strasbg.fr/viz-bin/qcat?J/A+A/520/A113

accuracy, ranging from a few tens of μas at magnitude 15−18 (target accuracies are 16 μas at 15 mag and 70 μas at 18 mag) to about 200 μas at magnitude 20 (Lindegren et al. 2008). Unlike Hipparcos, Gaia will permit the realization of the extragalactic reference frame directly at optical bands, based on the QSOs which have the most accurate positions (e.g. those with magnitudes brighter than 18, as suggested by Mignard 2003). Simulations show that the residual spin of the Gaia frame can be determined to 0.5 μas/yr with a "clean sample" of at least 10 000 of these sources (Mignard 2002). A preliminary Gaia catalog is expected to be available by 2015 with the final version released by 2020.

In the future, aligning the Gaia frame and the VLBI frame (i.e. the ICRF2, or any successor introduced by 2015) will be crucial for ensuring consistency between measured radio and optical positions. This alignment will be important not only for guaranteeing a proper transition if the fundamental reference frame is moved from the radio to the optical domain, but also for registering the radio and optical images of any celestial target with the highest accuracy. Such a registration will allow one, for example, to pinpoint the relative location of the optical and radio emission in active galactic nuclei (AGN) to a few tens of μas, placing constraints on the overall AGN geometry. Recent estimates of this optical-radio core shift indicate that it amounts to ∼150 μas on average at X-band (Kovalev et al. 2008), significantly larger than Gaia and VLBI position accuracies. It should thus be directly measurable. Conversely, these shifts will also affect the accuracy of the link between the two frames. For this reason a large number of objects is desirable in order to average out such effects.

The alignment between the VLBI and Gaia frames also requires sources with very accurate radio and optical positions. This implies that the link sources must be optically-bright (brighter than magnitude 18, as mentioned above) and not show any extended VLBI structures in order to ensure the highest VLBI astrometric accuracy (Fey & Charlot 2000). In a previous study we investigated possibilities of alignment based on the list of ICRF sources (Bourda et al. 2008). This study showed that, although about 30% of the ICRF sources have an optical counterpart brighter than magnitude 18, only one third of these are compact enough on VLBI scales. Overall, only 70 ICRF sources (10% of the catalog) were found to be appropriate for the alignment with the future Gaia frame. This highlights the need to identify additional suitable radio sources. Searching for such new sources implies going to weaker flux densities, thereby requiring the use of sensitive VLBI networks such as the European VLBI Network (EVN).

This paper gives an overview of the multi-step VLBI observing project that we have devised to identify further suitable sources for accurately aligning the radio and the future Gaia frames. It also presents results from initial observations. The strategy for selecting the sources is presented in Sect. 2.1 and the three successive steps of the project are explained in Sect. 2.2. The initial two experiments carried out in June and October 2007 are detailed in Sect. 3, and their analysis is described in Sect. 4. Finally, the VLBI results are discussed in terms of source detection rate and flux density in Sect. 5.

2. Multi-step VLBI observing program

2.1. Source selection

For this project the choice was made to search for additional radio sources suitable for aligning the VLBI and Gaia frames by observing new VLBI sources. As mentioned above, this implies going to radio sources weaker than those observed so far with geodetic VLBI. For this the NRAO VLA Sky Survey (NVSS; Condon et al. 1998) was used. This is a dense catalog of radio sources (about 2 000 000 sources observed at 1.4 GHz), derived from a deep radio survey (complete to the 2.5 mJy level), which covers the entire sky north of −40° (about 82% of the sky).

To identify new radio sources that have a suitable optical counterpart (i.e. brighter than magnitude 18) we have cross-identified the positions in this catalog with those in the Véron-Cetty & Véron (2006) optical catalog of QSOs. From these results, we excluded the ICRF and VCS sources. Cross-identification of the VCS with an optical catalog is the subject of a separate study to be presented elsewhere. Cross-identification with the ICRF has already been done and the results are presented in Bourda et al. (2008). For cross-identifying the NVSS with the Véron-Cetty & Véron (2006) optical catalog it was necessary to set an upper limit on the optical-radio position differences, above which radio and optical sources were considered to be different objects. We decided to adopt an upper limit of 3″, equivalent to three times the accuracy of the optical and radio positions in these catalogs, which is roughly at the 1″ level.

Following this cross-identification, additional criteria were adopted to limit the sample obtained. First, a lower declination limit $\delta \geq -10°$ was adopted to make possible observing with northern VLBI arrays. Additionally, the radio sources should be strong enough to be detectable in S/X type observations. In practice, this limits the flux density of the targets to about 20 mJy (at 1.4 GHz), assuming a VLBI data rate of 1 Gb/s and the use of large antennas such as Effelsberg.

The final sample consists of all NVSS survey sources with declination ≥−10°, flux density ≥20 mJy at 1.4 GHz, and identified with a QSO brighter than 18 mag in the catalog of Véron-Cetty & Véron (2006). These criteria result in a total of 447 weak extragalactic radio sources, most of which have never been observed with VLBI before.

2.2. Observing strategy

Observing these weak radio sources requires the use of a very sensitive VLBI network. Moreover, the sources detected need to be point-like on VLBI scales in order to permit precision VLBI astrometry. And finally, dedicated VLBI astrometric measurements will be necessary to achieve the highest accuracy in the alignment of the future Gaia frame with the radio reference frame. Accordingly, our observing strategy for identifying suitable link sources in the sample described above comprises three successive steps, which are:

1. **VLBI detection**: this step is dedicated to assessing the VLBI detectability of the 447 weak extragalactic radio sources and to obtaining estimates of their flux densities on VLBI scales.
2. **VLBI imaging**: this second step is aimed at imaging the sources detected in step 1, in order to investigate their VLBI structures and identify the most compact ones.
3. **VLBI astrometry**: this final stage is devoted to determining accurate VLBI positions (< 100 μas) for the most point-like sources identified in step 2.

In order to be detected with VLBI, a radio source should possess a compact component on VLBI scales. Following Porcas et al. (2004), one might expect that at least one-third of all sources should meet this criterion. It is expected, however, that many more should qualify in the present sample because of our initial quasar selection and because many candidates are also part of the

Table 1. Estimates of the minimum flux density detectable at X and S-bands for the baselines used for EC025A and EC025B (Eb = Effelsberg, Mc = Medicina, Nt = Noto, On = Onsala, Ro = Robledo), for geodetic-style, dual-frequency S/X observations recorded at 1 Gb/s during 5-min long scans. A radio source is considered detected if the $SNR \geq 7$.

	Minimum flux density detectable (mJy)									
	Eb–Mc	Eb–Nt	Eb–On	Mc–Nt	Mc–On	Nt–On	Eb–Ro	Mc–Ro	Nt–Ro	On–Ro
X-band	3	5	5	25	29	45	0.7	4	6	7
S-band	13	17	21	28	32	47	3	5	6	8

Sloan Digital Sky Survey (SDSS; Abazajian et al. 2009); it has been found, for example, that about 80% of SDSS quasars are detectable on VLBI scales (Frey et al. 2008). Candidate sources should, in addition, not show significant extended emission on VLBI scales, in order to limit the impact of so-called "source structure effects" and hence permit highly-accurate VLBI astrometry. It has been found that about 40% of the ICRF sources satisfy this condition (Charlot et al. 2006). Assuming the same fraction in our sample, one can expect another ~150 additional radio sources suitable for accurately aligning the VLBI and Gaia frames, which would more than triple the number of such sources compared to those available today.

3. Initial VLBI observations and data reduction

The first stage of the project described above was performed during two 48-hour experiments conducted on 2007 June 18 and 2007 October 26 (designated EC025A and EC025B, respectively). The observations were made with a network of four EVN telescopes (Effelsberg, Medicina, Noto, Onsala) and also the 70 m Robledo telescope for part of the time in EC025B, recording at 1 Gb/s in a geodetic-style dual-frequency S/X (13/3.6 cm) mode. These observations were carried out with a reduced network (6−10 baselines) since the goal was only to assess the detectability of the sources on VLBI scales. In theory a single baseline would be sufficient for this purpose but, for reasons of sensitivity (see Sect. 4) and redundancy, more than two telescopes were used. The maximum angular resolution, obtained with the baseline Noto-Onsala, is about 4 mas at X-band and 14 mas at S-band.

We chose to first observe those sources from the sample that belong to the CLASS catalog (Myers et al. 2003) in order to maximize the chances of detection during the initial experiment, since this catalog is known to be composed of compact sources (i.e. sources with relatively flat radio spectra). From the original sample, we identified 234 sources belonging to the CLASS catalog but, because of scheduling constraints, we could not fit all the CLASS sources in the initial experiment. Consequently, 208 sources from CLASS were observed during EC025A, together with 10 additional sources. The remaining 229 sources were observed during EC025B.

The purpose of these two experiments was to determine the VLBI detectability of the 447 weak extragalactic radio sources in our sample, based on snapshot observations. Each source was observed for two 5-min scans widely separated in time. Overall, the schedule for each experiment comprised 10 scans per hour (leaving 10 min for slewing between sources), and was optimized to minimize the telescope slewing time from source to source. No attempt was made to optimize the sky coverage above each telescope (as usually done for astrometry and geodesy experiments) since astrometric accuracy was not the motivation at this initial stage. For this reason the recording time at each telescope was about 80% of the total duration of the experiments (compared to less than 50% in standard geodetic VLBI experiments).

The data were correlated with the MkIV correlator at MPIfR (Max Planck Institute for Radio Astronomy) in Bonn (Germany). After correlation, post-processing was conducted with the fringe-fitting program *fourfit*[1] of the HOPS package (Whitney et al. 2004).

4. Results

The fringe-fitted data were analyzed in two ways. In the first we examined the signal-to-noise ratio (SNR) for each source on each baseline. A source is considered detected if it has a $SNR \geq 7$ on at least one baseline for at least one scan. Based on a 5-min on-source integration time with S/X dual-frequency observations recorded at 1 Gb/s, one can estimate the minimum flux density detectable at X and S-bands. Table 1 shows the sensitivity detection thresholds on the various baselines. Some baselines are much more sensitive than others and, for this reason, a source may be detected on some, but not all, baselines. For instance, in theory the minimum flux density that can be detected on the baseline Effelsberg-Medicina (the most sensitive in EC025A) is 3 mJy at X-band and 13 mJy at S-band. However, during the periods in EC025B when the Robledo telescope was observing, the minimum flux density that can be detected on the baseline Effelsberg-Robledo is ~700 μJy at X-band and 3 mJy at S-band.

In the second analysis we derived the mean correlated flux densities at S and X-bands for the detected targets, averaging over all baselines with $SNR \geq 7$ and using a rough calibration scheme. The latter was based on a priori gain curves and system temperature measurements for each antenna. The detection rates resulting from this analysis are summarized in Table 2:

- 432 sources were detected at X-band, corresponding to a detection rate of 97%;
- 399 sources were detected at S-band, corresponding to a detection rate of 89%.

Except for one source, all sources detected at S-band were also detected at X-band (398 sources), corresponding to a detection rate of 89%. This is in agreement with the results reported in Frey et al. (2008) for quasars from the SDSS (80%). The distribution of these sources on the sky is also plotted in Fig. 1.

The distributions of the mean correlated flux densities have median values of 26 mJy at X-band and 46 mJy at S-band (see Fig. 2), with the weakest sources at a level of 1 mJy at X-band and 8 mJy at S-band. The results for the 398 sources detected at both frequencies are available at CDS. Table 3 shows a sample of sources extracted from this list and Table 4 details the results for the sources that were not detected in one or both bands. These two tables give the names and coordinates of the sources observed during EC025A and EC025B, the optical magnitude,

[1] http://www.haystack.mit.edu/tech/vlbi/hops.html

Table 2. VLBI detection rates for the 447 weak extragalactic radio sources observed during EC025A and EC025B. In this study, *detection* means that at this frequency the $SNR \geq 7$, for at least one scan on one baseline.

	Sources observed	*X*-band detection	*S*-band detection	*S* and *X* detection
EC025A	218	216 sources 99%	211 sources 96%	211 sources 96%
EC025B	229	216 sources 94%	188 sources 82%	187 sources 82%
Overall	447	432 sources 97%	399 sources 89%	398 sources 89%

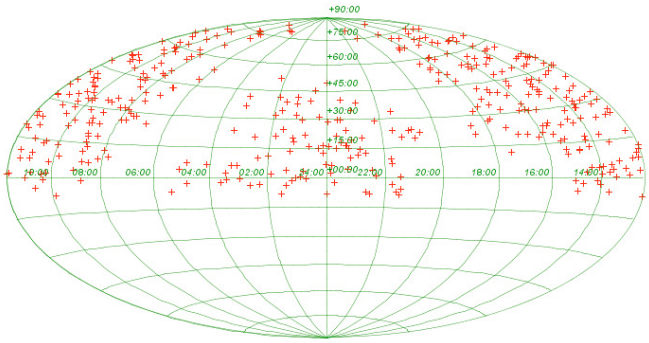

Fig. 1. Sky distribution of the 398 weak extragalactic radio sources detected at both *S* and *X*-band with the EVN during EC025A and EC025B (graph obtained with the tool *topcat*; Tool for OPerations on Catalogues And Tables; http://www.star.bris.ac.uk/~mbt/topcat.

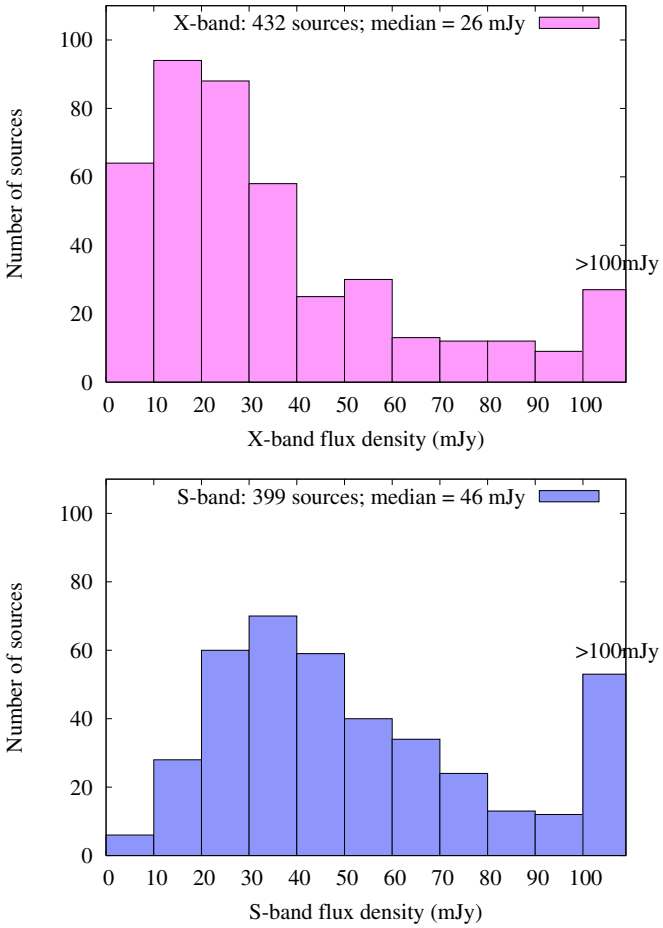

Fig. 2. Mean correlated flux density distribution, at *X* and *S*-bands, for the sources detected in EC025A and EC025B. The corresponding median values are 26 mJy and 46 mJy, respectively.

redshift, and type of object as extracted from the catalog of Véron-Cetty & Véron (2006), and the *S*- and *X*-band mean correlated flux densities determined from these observations. The third column lists the name of the catalog from which the source coordinates have been extracted. Coordinates from the NVSS catalog itself are only accurate to 1″ so, where possible, more precise coordinates from other catalogs have been given.

Figure 3 shows a comparison between the *X*-band flux density distribution for our sources, and those from the VCS and ICRF catalogs. The median flux density is 27 times weaker than for the ICRF sources and 8 times weaker than for the VCS sources.

The spectral index α_{SX} (defined as $S \propto \nu^{\alpha_{SX}}$, where S is the source flux density and ν is the frequency) was also investigated. α_{SX} was calculated using Eq. (1):

$$\frac{S\text{-band mean correlated flux density}}{X\text{-band mean correlated flux density}} = \left(\frac{2.3}{8.4}\right)^{\alpha_{SX}}. \quad (1)$$

Figure 4 shows the spectral index distribution for the 398 radio sources detected at both frequencies. The distribution for those which also belong to the CLASS catalog, which is composed of compact sources, is also plotted and no major differences are apparent. The median value of α_{SX} is −0.34. About 70% of the sources have $\alpha_{SX} > -0.5$ (274 out of 398 sources), indicating that they are likely to have a dominating core component, which promises well for future stages of this project.

5. Discussion

This paper has reported about VLBI detection observations, undertaken within the framework of a more global program dedicated to defining a new sample of radio sources suitable for the alignment of the radio celestial reference frame with the future Gaia frame.

First we discuss the selection of these weak extragalactic radio sources. The sample of sources to observe with VLBI was carefully selected in order to ensure a subsequent accurate Gaia position. Since the NVSS radio catalog used contains all possible weak sources, the main selection criterion was in limiting the apparent magnitude of their optical counterparts to brighter than 18. However, AGN are known to exhibit structural and flux-density variability at radio bands, and variable optical magnitudes. Some sources may therefore become too faint, and hence unsuitable for the alignment, before or during the Gaia mission. Accordingly, it seems necessary to envision future optical monitoring of the sources before final selection of those to be used to align the radio and the optical frames.

Ultimately, the sources selected for the VLBI-Gaia alignment should be distributed uniformly on the sky, in order to avoid any systematic effects. However, the sample selected by our project is limited to declinations above −10° since the VLBI arrays, and hence our VLBI observations, are concentrated in the Northern hemisphere (see Fig. 1 which illustrates the discrepancy between Northern and Southern hemisphere coverage). The Asia Pacific Telescope (APT; Gulyaev & Natusch 2007) can, from now on, play a significant role, and analogous observations of weak extragalactic radio sources in the Southern hemisphere

Table 3. Sample of 15 sources extracted from the list of 398 extragalactic radio sources detected during EC025A and EC025B experiments (211 out of 218 detected during EC025A, and 187 out of 229 detected during EC025B). The complete list is available at the CDS.

IERS name	Name from catalog	Catalog	V	z	Type	α			δ			Flux		α_{SX}	Exp.
						h	min	s	°	′	″	S	X		
0946+091	09480+08421I	FIRST	17.49	1.971	QUA	9	48	53.6070	8	55	14.410	16	3	−1.28	B
0949+241	GB6J095207+235248	CLASS	16.78	0.970	QUA	9	52	6.3897	23	52	45.250	30	18	−0.39	A
0948+658	095232+653800	NVSS	18.00		BL	9	52	32.2300	65	38	0.300	34	30	−0.08	B
0950−084	J095301−084034	CRATES	17.20		BL	9	53	2.7200	−8	40	18.400	62	48	−0.20	A
0950+326	GB6J095328+322552	CLASS	17.74	1.574	QUA	9	53	27.9563	32	25	51.530	71	133	0.48	A
0952+338	GB6J095537+333522	CLASS	17.44	2.500	QUA	9	55	37.9383	33	35	3.937	66	46	−0.28	A
0956+216	095930+212319	NVSS	17.40	0.365	BL	9	59	30.0400	21	23	19.200	18	15	−0.18	B
0957+136	GB6J100035+132440	CLASS	17.15	1.352	QUA	10	0	33.8516	13	24	10.896	50	21	−0.67	A
0957+561*	GB6J100121+555357	CLASS	16.98	1.413	QUA	10	1	20.6911	55	53	55.611	24	11	−0.60	A
0959+684	GB6J100308+681313	CLASS	15.92	0.773	QUA	10	3	6.7676	68	13	16.811	57	31	−0.47	A
1002+483	10060+47544F	FIRST	17.65	2.370	QUA	10	5	15.9610	48	5	33.210	50	18	−0.80	B
1001+621	GB6J100516+615443	CLASS	17.81	2.740	QUA	10	5	17.6044	61	54	17.281	36	13	−0.79	A
1007+716	GB6J101132+712434	CLASS	17.60	1.192	QUA	10	11	32.6159	71	24	41.616	466	42	−1.86	A
1009+334	GB6J101211+330936	CLASS	17.99	2.260	QUA	10	12	11.4526	33	9	26.414	70	47	−0.31	A
1009+067	GB6J101213+063051	CLASS	16.80	0.727	BL	10	12	13.3477	6	30	57.175	83	62	−0.23	A

Notes. The apparent optical magnitude from Véron-Cetty & Véron (2006) is denoted V, the redshift z, and the type of the object is "BL" for BL Lac objects and "QUA" for quasars. The right ascension α and declination δ are extracted from the catalog specified in the third column. The mean correlated flux densities are given in mJy, the derived S/X spectral index is denoted α_{SX}, and the name of the experiment is given in the last column ("A" for EC025A and "B" for EC025B).
IERS name of gravitational lenses is marked with an asterisk. These sources will be omitted from subsequent steps of the project.
The catalogs from which the coordinates were extracted are: CLASS (Myers et al. 2003; position accuracy ∼35 mas), CRATES (Healey et al. 2007; position accuracy ranging from ∼50 mas to 1″), FIRST (Becker et al. 1995; position accuracy ranging from ∼50 mas to 1″), NVSS (Condon et al. 1998; position accuracy ∼1″), and AHA (Andrei, A. H. 2007, private communication of improved positions for QSOs as extracted from the input catalog for Gaia; position accuracy better than 1″). For the last catalog, the name of the source written in the table is extracted from Véron-Cetty & Véron (2006).

will be planned within the next few years. Figure 1 also highlights the gap in the source distribution within the galactic plane, which is due to galactic extinction at optical wavelengths.

During the post-processing analysis of EC025A and EC025B, mean correlated flux densities at S and X-bands were determined for each source detected (see Sect. 4). A strong but partially-resolved source may be detected on all baselines and hence the average correlated flux density will be less than the total flux density. However, a weaker source may become *undetected* on baselines where it is resolved, so the average correlated flux density could be nearer to the total flux density. Accordingly, the "mean correlated flux densities" (and the spectral index α_{SX} derived from them) are biased estimates. However, this is not so important since their main use is as indicators as part of the selection process for further observations.

By examining the results in detail it can be seen that the lowest flux densities detected during the two experiments are quite close to the theoretical sensitivity thresholds given in Table 1 (3 mJy at X-band and 13 mJy at S-band during EC025A; 0.7 mJy at X-band and 3 mJy at S-band during EC025B). The minimum flux densities detected during EC025A were ∼6 mJy at X-band and ∼21 mJy at S-band; during EC025B they were ∼1 mJy at X-band and ∼8 mJy at S-band. Table 2 shows the difference between the detection rates during EC025A (96%) and EC025B (82%). This can be explained by the source selection process. The first experiment, EC025A, was mainly composed of sources from the CLASS catalog, a survey of compact sources as mentioned above. Accordingly, the VLBI detection rate is higher than during EC025B, which was composed of sources from other radio surveys.

Figure 5 compares the S-band mean correlated flux density distributions for the sources detected in EC025A and EC025B. One can note that, during EC025A, in contrast to EC025B, no source with a flux density below 20 mJy was detected at S-band, demonstrating that the detectability of the sources clearly depends on the VLBI array (see Sect. 4 and Table 1). The reason is that the only highly-sensitive antenna involved in EC025A was the 100 m-diameter Effelsberg telescope, which has a limited S-band sensitivity, with a system noise temperature of ∼80 K, compared to ∼40 K for the 30 m-diameter Medicina telescope. During EC025B the 70 m-diameter Robledo antenna joined the network for some of the time, which significantly increased the number of detections for the weakest sources. Thus the S-band detection rate is non-uniform over the sample.

Finally, even though the only selection criterion applied to the NVSS radio catalog was the optical magnitude cut-off ($V \leq 18$), one should note the high overall detection rate obtained (89%). This implies that optically-bright radio sources have compact structures on VLBI scales. This result confirms previous findings (Frey et al. 2008) and is very important for future VLBI experiments and astrophysical studies (e.g. correlation of optical brightness with the direction of the radio jet).

6. Conclusion

Based on observations with the European VLBI Network, we have identified 398 VLBI sources (most of them never observed with VLBI before) which are potential candidates for the future alignment of the radio and Gaia frames. The median flux density of these sources is 27 times weaker than that of the ICRF sources. This new sample increases significantly the current number of potential VLBI-Gaia link sources. The adoption of the ICRF2 (containing data from the VCS catalogs) as the new IAU fundamental celestial reference frame also provides a natural opportunity for us to identify additional radio sources suitable for this alignment.

Table 4. List of the 49 extragalactic radio sources not detected in one or both bands during EC025A and EC025B (7 sources out of 218 observed during EC025A and 42 sources out of 229 observed during EC025B).

IERS name	Name from catalog	Catalog	V	z	Type	α			δ			Correlated flux		Exp.
						h	min	s	°	′	″	S-band	X-band	
0015+160	001831+162042	NVSS	17.68	1.333	QUA	00	18	31.3300	16	20	42.000	–	2	B
0017+154	002025+154052	NVSS	17.65	2.018	QUA	00	20	25.3200	15	40	52.700	–	–	B
0106+149	SDSS J01090+1512	AHA	17.81	0.381	QUA	01	09	00.3756	15	12	17.611	–	5	B
0109+380	GB6J011216+381910	CLASS	17.30	0.331	QUA	01	12	18.0551	38	18	56.852	–	–	A
0123+349	012555+351036	NVSS	16.42	0.312	QUA	01	25	55.9200	35	10	36.700	–	2	B
0146+294	GB6J014913+294230	CLASS	16.80	0.340	QUA	01	49	12.4255	29	42	29.652	–	8	B
0157+001	01585+00130E	FIRST	15.90	0.163	QUA	01	59	50.2480	00	23	40.980	–	–	B
0804+480	080814+475242	NVSS	17.99	0.545	QUA	08	08	14.4900	47	52	42.300	–	4	B
0813−074	081604−073557	NVSS	16.10	0.040	BL	08	16	04.3600	−07	35	57.100	–	–	B
0844+117	GB6J084710+113424	CLASS	16.90	0.198	BL	08	47	12.9346	11	33	50.167	–	6	A
0850+536	GB6J085416+532731	CLASS	17.50	2.418	QUA	08	54	17.6145	53	27	35.200	–	14	A
0902+058	09060+05386I	FIRST	17.90	1.216	QUA	09	05	07.4670	05	37	17.420	–	6	B
0924+606	GB6J092841+602512	CLASS	17.23	0.295	QUA	09	28	37.9939	60	25	20.988	–	4	A
0944+540	09480+53420G	FIRST	16.97	0.492	QUA	09	47	56.0140	53	50	00.440	8	–	B
0946+319	09480+31430E	FIRST	17.30	0.309	QUA	09	49	27.6800	31	41	09.960	–	–	B
0952+457	095539+453214	NVSS	16.94	0.259	QUA	09	55	39.9400	45	32	14.600	–	4	B
0957+227	4C 22.25	AHA	18.00	0.419	QUA	10	00	21.8021	22	33	18.720	–	2	B
1019+397	10240+39393E	FIRST	17.63	0.605	QUA	10	22	37.4160	39	31	50.540	–	17	B
1045+388	104807+383736	NVSS	17.58	0.600	QUA	10	48	07.5400	38	37	36.500	–	8	B
1101+216	GB6J110434+212411	CLASS	16.40	0.188	QUA	11	04	36.3439	21	24	17.996	–	9	A
1103−006	11060−00520G	FIRST	16.46	0.426	QUA	11	06	31.7780	00	52	51.920	–	90	B
1132+262	GB6J113456+255531	CLASS	17.60	0.714	QUA	11	34	57.6265	25	55	27.903	–	11	A
1143+280	GB6J114631+274605	CLASS	18.10	0.314	QUA	11	46	31.6809	27	46	24.203	–	22	B
1146+111	MC 1146+111	AHA	17.99	0.863	QUA	11	48	47.8414	10	54	58.536	–	1	B
1217−029	12210−03020G	FIRST	17.95	0.299	BL	12	19	45.6950	−03	14	24.060	–	10	B
1218+086	12210+08158I	FIRST	17.10	0.132	BL	12	21	32.0590	08	21	44.070	–	15	B
1222+320	12240+31430E	FIRST	18.00	1.274	QUA	12	25	16.9700	31	45	35.010	–	5	B
1230−002	J123303−003051	CRATES	17.90	0.470	QUA	12	33	04.0500	00	31	34.200	–	–	A
1237+353	124021+350259	NVSS	17.24	1.194	QUA	12	40	21.2300	35	02	59.300	–	18	B
1241+154	12450+15180I	FIRST	18.10	1.395	QUA	12	43	44.8370	15	08	20.600	–	7	B
1253+626	GB6J125506+622055	CLASS	18.05	1.978	QUA	12	55	08.0898	62	20	50.423	–	9	B
1255+370	12570+36364E	FIRST	17.80	0.709	QUA	12	57	23.8630	36	44	19.390	–	–	B
1323+004	13270+00260G	FIRST	15.80	0.082	BL	13	26	17.4570	00	13	22.860	–	–	B
1351+000	13540−00260G	FIRST	16.80	1.504	QUA	13	54	25.2240	00	13	57.990	–	–	B
1358+594	RXS J13598+5911	AHA	18.09	0.689	BL	13	59	53.7869	59	11	03.005	–	4	B
1430−007	14330−00520G	FIRST	17.52	1.023	QUA	14	32	44.4660	00	59	14.980	–	–	B
1449+342	14510+34082E	FIRST	18.00	0.484	QUA	14	51	31.9220	34	02	32.030	–	2	B
1600+091	16030+09084I	FIRST	17.30	0.488	QUA	16	03	17.8040	09	00	38.030	–	8	B
1624+349	16270+34376E	FIRST	18.00	1.337	QUA	16	26	20.4650	34	51	43.160	–	2	B
1636+715	GB6J163551+712847	CLASS	15.84	0.171	QUA	16	35	52.1118	71	28	53.835	–	16	B
1651+402	16540+40104E	FIRST	17.00	0.148	BL	16	52	53.2950	40	09	12.870	–	–	B
1700+518	17000+51396F	FIRST	15.12	0.292	QUA	17	01	24.8980	51	49	20.380	–	3	B
1937−007	J194008−003848	CRATES	18.10	1.711	QUA	19	40	9.0000	00	39	02.100	–	–	B
2052−005	205528−002115	NVSS	18.07		BL	20	55	28.2300	00	21	15.800	–	–	B
2120+168	3C 432.0	AHA	17.96	1.785	QUA	21	22	46.3308	17	04	38.125	–	3	B
2127+176	TEX 2127+176	AHA	18.00	2.010	QUA	21	29	38.1907	17	54	46.159	–	24	B
2143−045	IRAS 21431−0432	AHA	15.70	0.103	QUA	21	45	45.7740	−04	18	04.259	–	–	B
2214+224	221710+223944	NVSS	17.80	0.405	QUA	22	17	10.9900	22	39	44.800	–	11	B
2302+368	230436+370507	NVSS	17.50		BL	23	04	36.6300	37	05	07.300	–	9	B

Notes. The apparent optical magnitude and redshift from Véron-Cetty & Véron (2006) are denoted V and z, respectively, and the object type is "BL" for BL Lac objects and "QUA" for quasars. The right ascension α and declination δ are extracted from the catalog specified in the third column. The S-band and X-band mean correlated flux densities are given in mJy, and "–" stands for a non-detection at this frequency. The last column specifies the experiment in which the source was observed ("A" for EC025A and "B" for EC025B).

The next step of the project described here is imaging the 398 sources at both frequencies using a global VLBI network (EVN+VLBA), in order to identify the most point-like sources and therefore those most suitable for the VLBI-Gaia alignment. Ultimately, the multi-step project described in this paper must demonstrate the feasibility of global VLBI astrometry with sub-milliarcsecond accuracy for targets that are typically fainter by one order of magnitude compared to ICRF sources. Additionally, it may also reveal whether fainter sources are more compact, and therefore more suitable than stronger sources for precision VLBI astrometry.

Within the next few years, the alignment between optical and radio frames will benefit from this multi-step VLBI project. Obtaining such an alignment with the highest accuracy

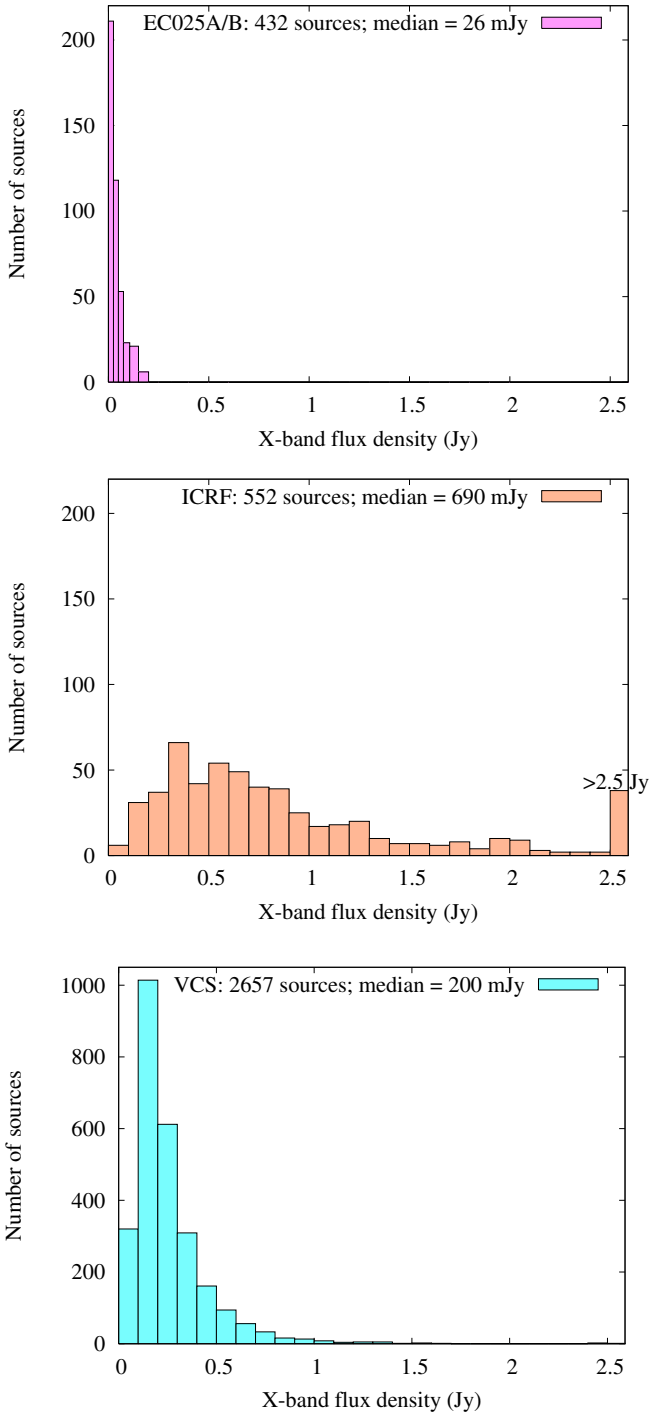

Fig. 3. Comparison of the X-band flux density distribution for the sources detected in EC025A and EC025B and those from the VCS and ICRF catalogs. The corresponding median values are 26 mJy, 200 mJy and 690 mJy, respectively. The number of VCS and ICRF sources corresponds to those with a published X-band flux density value.

is essential, not only to ensure consistency between measured radio and optical positions, but also to measure directly core shifts within AGNs. This will be of great interest in the future for probing AGN jets properties.

Acknowledgements. The authors would like to thank the VLBI friends at the five EVN observing stations (Effelsberg, Medicina, Noto, Onsala and Robledo), Dave Graham and Walter Alef for assistance with the correlation in Bonn,

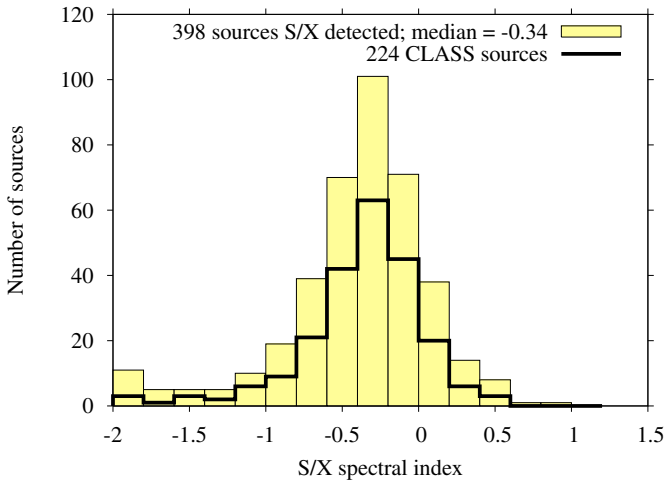

Fig. 4. S/X spectral index distribution for the 398 weak extragalactic radio sources detected at both S and X-bands during the experiments EC025A and EC025B. The S/X spectral index distribution for the sources also belonging to the CLASS catalog is plotted.

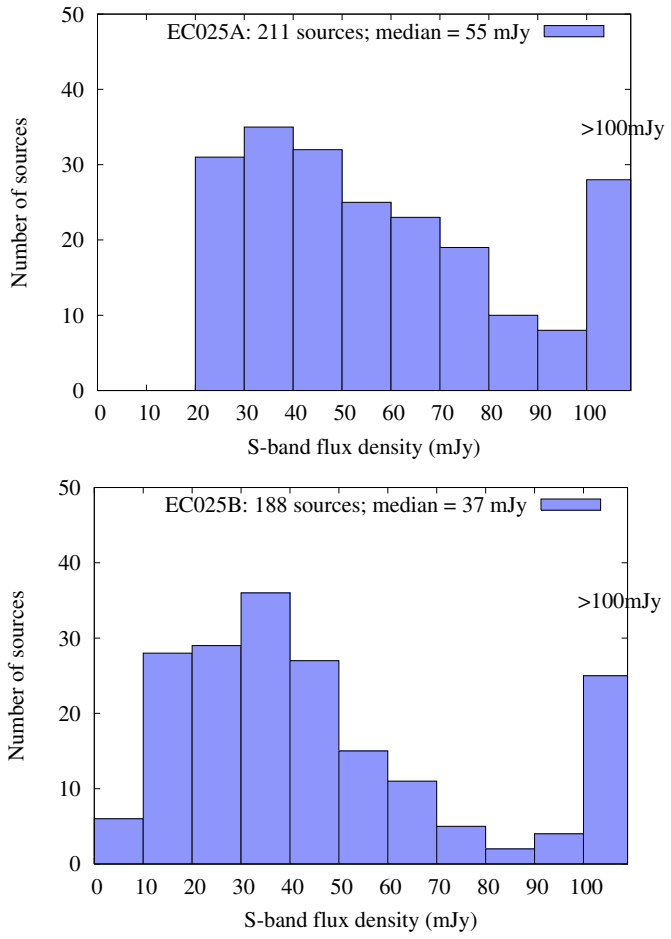

Fig. 5. Mean correlated flux density distribution at S-band for the sources detected in EC025A (*upper panel*) and EC025B (*lower panel*). The corresponding median values are 55 mJy and 37 mJy, respectively. For the sources with S-band mean correlated flux density below 20 mJy, there are no detections during EC025A, whereas there are for EC025B.

John Gipson for advice when scheduling the observations, and Alexander Andrei for providing improved positions for some sources in our sample. This work has benefited from research funding from the European Community's sixth Framework Programme under RadioNet R113CT 2003 5058187. The EVN is a joint facility of European, Chinese, South African and other radio astronomy institutes funded by their national research councils. Finally, the first author is grateful to the CNES (Centre National d'Études Spatiales, France) for the post-doctoral position granted at Bordeaux Observatory between October 2006 and September 2008.

References

Abazajian, K. N., Adelman-McCarthy, J. K., Agüeros, M. A., et al. 2009, ApJS, 182, 543
Arias, E. F., Charlot, P., Feissel, M., & Lestrade, J.-F. 1995, A&A, 303, 604
Beasley, A. J., Gordon, D., Peck, A. B., et al. 2002, ApJS, 141, 13
Becker, R. H., White, R. L., & Helfand, D. J. 1995, ApJ, 450, 559
Bourda, G., Charlot, P., & Le Campion, J.-F. 2008, A&A, 490, 403
Charlot, P., Fey, A. L., Ojha, R., & Boboltz, D. A. 2006, in International VLBI Service for Geodesy and Astrometry 2006, General Meeting Proceedings, ed. D. Behrend, & K. D. Baver, NASA/CP-2006-214140, 321
Condon, J. J., Cotton, W. D., Greisen, E. W., et al. 1998, AJ, 115, 1693
Fey, A. L., & Charlot, P. 2000, ApJS, 128, 17
Fey, A. L., Ma, C., Arias, E. F., et al. 2004, AJ, 127, 3587
Fomalont, E. B., Petrov, L., MacMillan, D. S., Gordon, D., & Ma, C. 2003, AJ, 125, 2562
Frey, S., Gurvits, L., Paragi, Z., et al. 2008, A&A, 477, 781
Gulyaev, S., & Natusch, T. 2007, in Astronomy for the Developing World, Special Session 5, ed. J. Hearnshaw, & P. Martinez, IAU XXVI, 53
Healey, S. E., Romani, R. W., Taylor, G. B., et al. 2007, ApJS, 171, 61
IERS Technical Note 35 2009, The Second Realization of the International Celestial Reference Frame by Very Long Baseline Interferometry (Frankfurt am Main: Verlag des Bundesamts für Kartographie und Geodäsie), ed. A. L. Fey, D. Gordon, & C. S. Jacobs
Kovalev, Y. Y., Petrov, L., Fomalont, E. B., & Gordon, D. 2007, AJ, 133, 1236
Kovalev, Y. Y., Lobanov, A. P., Pushkarev, A. B., & Zensus, J. A. 2008, A&A, 483, 759
Ma, C., Arias, E. F., Eubanks, T. M., et al. 1998, AJ, 116, 516
Lindegren, L., Babusiaux, C., Bailer-Jones, C., et al. 2008, in A Giant Step: from Milli- to Micro-arcsecond Astrometry, ed. W. J. Wenjin, I. Platais, & M. A. C. Perryman (Cambridge University Press), IAU Symp. Proc., 248, 217
Mignard, F. 2002, in Gaia: A European Space Project, ed. O. Bienaymé, & C. Turon, EAS Publ. Ser., 2, 327
Mignard, F. 2003, in The International Celestial Reference System: Maintenance and Future Realization, ed. R. Gaume, D. McCarthy, & J. Souchay, Joint Discussion 16, IAU XXV, 133
Myers, S. T., Jackson, N. J., Browne, I. W. A., et al. 2003, MNRAS, 341, 1
Perryman, M. A. C., de Boer, K. S., Gilmore, G., et al. 2001, A&A, 369, 339
Petrov, L., Kovalev, Y., Fomalont, E., & Gordon, D. 2005, AJ, 129, 1163
Petrov, L., Kovalev, Y., Fomalont, E., & Gordon, D. 2006, AJ, 131, 1872
Petrov, L., Kovalev, Y., Fomalont, E., & Gordon, D. 2008, AJ, 136, 580
Porcas, R., Alef, W., Ghosh, T., Salter, C. J., & Garrington, S. T. 2004, in 7th European VLBI Network Symposium Proceedings, OAN, Madrid, ed. R. Bachiller, F. Colomer, J.-F. Desmurs, & P. de Vicente, 31
Véron-Cetty, M.-P., & Véron, P. 2006, A&A, 455, 773
Whitney, A. R., Cappallo, R., Aldrich, W., et al. 2004, Radio Sci., 39, RS1007